Taylor & Francis
Taylor & Francis Group

Automatika

Journal for Control, Measurement, Electronics, Computing and Communications

ISSN: (Print) (Online) Journal homepage: https://www.tandfonline.com/loi/taut20

A novel salp swarm assisted hybrid maximum power point tracking algorithm for the solar photovoltaic power generation systems

M. Premkumar, C. Kumar, R. Sowmya & J. Pradeep

To cite this article: M. Premkumar, C. Kumar, R. Sowmya & J. Pradeep (2021) A novel salp swarm assisted hybrid maximum power point tracking algorithm for the solar photovoltaic power generation systems, Automatika, 62:1, 1-20, DOI: 10.1080/00051144.2020.1834062

To link to this article: https://doi.org/10.1080/00051144.2020.1834062

Published online: 23 Oct 2020.

AUTOMATIKA
2020, VOL. 62, NO. 1, 1–20
https://doi.org/10.1080/00051144.2020.1834062

A novel salp swarm assisted hybrid maximum power point tracking algorithm for the solar photovoltaic power generation systems

M. Premkumar [a], C. Kumar [b], R. Sowmya [c] and J. Pradeep [d]

[a]Department of Electrical and Electronics Engineering, GMR Institute of Technology, Rajam, India; [b]Department of Electrical and Electronics Engineering, M. Kumarasamy College of Engineering, Karur, India; [c]Department of Electrical and Electronics Engineering, National Institute of Technology, Tiruchirapalli, India; [d]Rajasthan Rajya Vidyut Prasaran Nigam, Sikar, India

ABSTRACT

The photovoltaic (PV) systems must work at the maximum power point (MPP) to derive the highest possible power with the higher performance during a change in operating conditions. The primary objective is to implement a novel hybrid tracking algorithm to extract the maximum output power from the solar PV panel or array under partial shading conditions (PSCs). This hybrid MPP tracking algorithm is based on the salp swarm algorithm (SSA), which finds the initial global peak (GP) operating point and is followed by the perturb and observation (P&O) algorithm in the last stage to realize a faster convergence rate. Thus, the computational burden met by the conventional methods such as standalone P&O, hybrid grey-wolf-optimization (HGWO), and hybrid whale-optimization algorithm (HWOA) algorithm reported in the literature is overcome by the proposed hybrid SSA algorithm called HSSA. The P&O algorithm searches the MPP in the projected search space by the SSA algorithm. The proposed hybrid algorithm is simulated using MATLAB/Simulink simulation tool to validate the effectiveness of tracking the MPP. The hybrid SSA is compared with the standalone P&O, hybrid WOA, and hybrid GWO, and from the simulation results, it is proved that the hybrid tracking algorithm exhibits a high tracking performance.

ARTICLE HISTORY
Received 12 July 2019
Accepted 30 September 2020

KEYWORDS
GP; hybrid GWO; hybrid WOA; MPP; partial shading condition; P&O; SSA

1. Introduction

Nowadays, renewable energy has been technologically advanced because it provides green and clean energy. Out of various renewable energy sources, the solar PV source plays a vital role in generating the clean and pure energy by transforming the solar photo energy to the electrical energy, and it is strengthened by the maximum power point tracking (MPPT) technique to produce the maximum possible power from the solar PV module [1,2]. The main objective of the MPPT technique is to locate the MPP to regularize the output voltage of the solar panel by controlling the converter operation [3,4]. The primary objective is to produce the highest power from the panel under a change in environmental conditions. This can be possible by adjusting the converter duty ratio and to locate the MPP [5,6]. The authors of [7,8] discussed various MPPT techniques for the PV based energy systems such as incremental conductance (IC), and perturb and observation (P&O), fractional open-circuit voltage, fractional short circuit current, modern MPPT techniques (based on neural network (NN), bio-inspired optimization, nature-inspired optimization, fuzzy logic (FL), etc.). The most familiar MPPT method is P&O, and it has several advantages such as simple structure, low cost, smooth implementation, and fewer parameters measurement. The MPPT controller alters the PV output power with a small step in each cycle, and this step size is kept fixed. The control parameters are PV voltage and PV current, and this is called perturbation. It depends on the power derivative concerning zero voltage at MPP. However, this method fails to locate the MPP under the fast-changing environmental condition, and its convergence speed is high [9,10]. These basic MPPT tracking algorithms are efficient only under consistent irradiance conditions. The conventional algorithms normally fail to track global peak for a system with PSC or rapid irradiance change, resulting in power losses of up to 70%. Furthermore, weather conditions, such as tropical conditions, can lead to rapid change in irradiance and PSC due to cloud, tree, dust, etc. This requires the quick tracking of the MPPT devices and the capability to track the global peak. The solar PV modules under PSCs are shown in Figure 1. During PSCs, the panel exhibits multiple local peaks (LP) and one global peak (GP), and it is very challenging to track the GP under PSCs, and conventional MPPT algorithms fail to track the GP [11].

The authors of [12] define the concept of an improved P&O MPPT algorithm for drift-free operations. A new variable step-size algorithm was proposed in [13] for an MPPT with fast-tracking characteristics

CONTACT M. Premkumar mprem.me@gmail.com Department of Electrical and Electronics Engineering, GMR Institute of Technology, Rajam, Andhra Pradesh, India

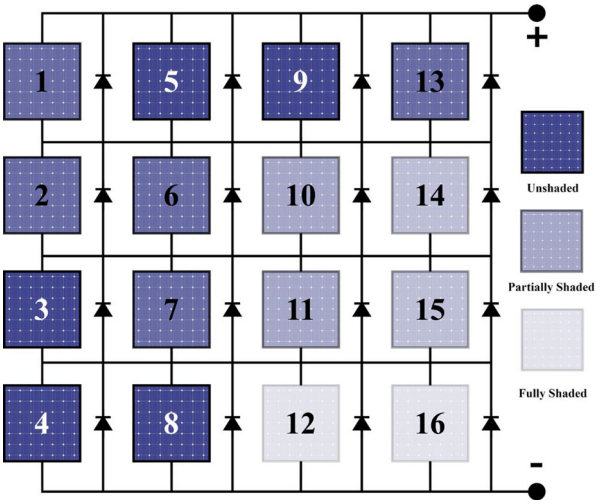

Figure 1. Solar PV array under PSCs.

and highly efficient during rapid irradiation changes. The authors of [14] presented a novel autoscaling variable step-size P&O MPPT technique to track the GP with less convergence speed. However, the maximum power generation is affected by the scaling factor (*S*), and the wrong selection of *S* leads to power oscillations. An IC technique was discussed in [15] to fulfil the MPPT goal during a change in insolation conditions. Another major aspect of research is the impact of PSC, where comprehensive studies are carried out in [16]. This result shows numerous PSC power peaks and requires an MPPT system that can differentiate between GP and LPs. In such cases, the conventional MPPTs may not be efficient; based on the PV array configurations and shading conditions, they can fall under LPs. So, a recent optimization algorithm neutralizes the PSCs effects by controlling the duty cycle of the converter. Soft computing-based bio-inspired optimization techniques such as artificial bee colony, bat optimizer, firefly, ant colony optimization, Particle Swarm Optimization (PSO) [17], flower pollination, Cuckoo search, etc. can track the GP effectively. However, the above-said algorithms exhibit oscillations under the steady-state condition, which makes the system ineffective. The algorithms, such as the bat algorithm and flower pollination, are addressed by [18] to track the GP, and flower pollination has high tracking efficiency than the bat algorithm. However, the algorithm fails to track the GP due to the less search space. The other meta-heuristic algorithms, such as Grey Wolf Optimization (GWO) [19], whale optimization algorithm (WOA) [20], harris-hawk optimization [21], slime mould algorithm [22], marine predator algorithm [23], salp-swarm optimization algorithm (SSA) [24], etc. were discussed in the literature. The GWO reduces the oscillation around the steady-state and improves the tracking efficiency with a good transient response. The WOA algorithm accurately locates the GP with a higher tracking speed and accuracy under PSCs. The WOA algorithm is better than the PSO and GWO in terms of accuracy and speed. To improve the steady-state performance, the GWO is combined with the conventional P&O algorithm, which also improves the tracking efficiency under a dynamic change in solar irradiation [25]. The initial stage of the change in insolation can be taken care of by the GWO, and the P&O controls the final stage. An artificial neural network (ANN) is combined with the P&O to reach a faster convergence rate, and it was proposed by [26]. At the initial stage, the ANN locates the GP, and finally, P&O locates the peak operating point by controlling the duty cycle of the converter. The WOA algorithm is combined with the P&O to reduce the steady-state oscillation with a better convergence rate under a change in operating conditions [27]. The WOA locates the GP at the initial stage, and the P&O algorithm finds the optimal operating point to achieve a higher convergence rate. To address the issues, such as tracking dynamic GP and large steady-state oscillation, is addressed by [28]. This paper proposed a hybrid PSO algorithm, in which the PSO takes care of the dynamic GP under various shading patterns, and the fuzzy logic controller (FLC) takes care of the steady-state oscillations. All the methods discussed in the literature do not guarantee that the shading pattern change due to the solar irradiation change or load variation. Moreover, the shading pattern may change when the search space is unchanged.

SSA is a new optimization algorithm to solve many problems of optimization with a single-objective and multi-objective [29]. The main drive of SSA is the swarming behaviour of salp as they swim and search for food in the oceans. This algorithm is mathematically modelled and tested on various benchmark functions in order to demonstrate their effective behaviours in finding the best solution for problem optimization. The authors of [30] have developed several metaheuristic algorithms, including SSA, to cope with automotive industry problems. The authors of [31] introduced an MPPT technique based on the SSA algorithm and tested with various operating conditions. The authors of [32] introduced an improved SSA to extract the solar cell parameters of the double-diode PV electrical model. The authors of [33] introduced a new version of the SSA tested for its efficiency by a number of common benchmark functions. The authors of [34] suggested a modern hybrid algorithm focused on a Sine Cosine with SSA and named as HSCSSA. The proposed hybrid technique improves the convergence execution with the exploitation and exploration of search spaces. Within the proposed technique, the SSA's position within the search space available is updated using the positions of the sine-cosine algorithm; thus, the best solutions are reserved based on sine or cosine. The authors of [35] implemented a new variant of the SSA based on Arctan transformation. This variant consists of two functional

characteristics, namely mobility and multiplicity, which improves the exploitation and exploration ability of SSA. The authors of [36] presented a multi-objective optimization based on hybrid SSA and Spotted Hyena Optimizer, named as HMOSHSSA. The HMOSHSSA utilizes the exploration capabilities of spotted hyena to examine the search space thoroughly, and the SSA is used to obtain the optimal solution, which can allow convergence quicker. Most of the metaheuristic algorithms in the literature have been trapped in local research and suffer from slow convergence [37]. The authors of [38] have introduced a new, improved SSA system. To enhance the performance of the SSA, opposition-based learning is presented in the conventional SSA. This algorithm is evaluated on various benchmark functions, and the performance is compared with optimization techniques. Many factors make it difficult to solve global problems of optimization: as dimensionality increases, the search regions increase exponentially, which is the key problem faced by most of the optimization methods [39]. Nevertheless, there is no theory to decide which algorithm gains the best efficiency; however, hybrid algorithms improve the performance of the basic algorithm [40]. For several problems of low and even medium dimensionality, the basic SSA has shown greater performance. Nevertheless, two main shortcomings are recognized in the basic SSA: lack of the solutions variety, which causes slow convergence and tenacious early convergence. Due to these limitations, SSA calls for additional improvement, modifying or hybridizing with other searching techniques, to avoid the early convergence to enhance the performance. The basic SSA has the merits of simple upgrading functionality but has the pitfalls to collapse into the local optimum with the multidimensional functions in particular. From the detailed literature, the shortcoming of the basic SSA is given as follows. (i) due to insufficient exploitation and exploration, it creates large output oscillations and (ii) less tracking speed.

Based on the literature, the above said bio-inspired optimization algorithms and the hybrid algorithms could able to locate the GP with high oscillations at a steady-state. Moreover, these techniques cannot track the dynamic GP under various shading patterns. Therefore, an improved hybrid technique called HSSA is proposed, and it is formulated by combining SSA and P&O to overcome the above-said problems. This HSSA algorithm improves the tracking efficiency with the high tracking speed under PSCs by controlling the duty cycle of the converter. The significant contributions to this research are as follows.

- A new hybrid HSSA is developed to track the MPP during PSCs
- The significant effects of the PSC are explained and validated
- The tracking efficiency of the HSSA during PSCs and rapid change in insolation is validated through simulation and experimentation
- The performance of HSSA is compared with the conventional P&O and few hybrid versions, such as HGWO and HWOA.

The rest of the paper is organized as follows: section 2 of the paper presents the solar photovoltaic panel mathematical modelling and its operating characteristics under PSCs. The modelling of the hybrid salp swarm algorithm and its usage to develop the MPPT control is illustrated in section 3. The simulation and experimental results are discussed in detail in section 4, along with the performance comparison among the various algorithms, as discussed in the literature. Finally, the paper is concluded in section 5.

2. Characteristics of the solar photovoltaic array

A photovoltaic array comprises multiple PV strings connected in parallel, each of which is constructed from different PV modules linked to each array, as shown in Figure 2. Each of the photovoltaic modules comprises several parallel and series-connected PV cells. A single PV cell's power is very limited and cannot be used for real-time applications, and the PV module is generally considered as a part of a single PV cell. Therefore, the characteristics of the PV panel are significant under various irradiance conditions, i.e. uniform irradiance and PSCs [41].

2.1. Uniform solar irradiation condition

Several researchers have presented various electric equivalent models to understand the output characteristics of a photovoltaic module. The single-diode model (SDM) is depicted in Figure 3. The paper opts for the most commonly encountered model due to its precise result and simple structure. The total current of a PV module can be represented according to the SDM as:

$$I = I_{ph} - I_0\left[exp\left(\frac{V_{pv} + IR_{se}}{nV_{th}}\right) - 1\right] - \left[\frac{V_{pv} + IR_{se}}{R_{sh}}\right] \quad (1)$$

Where n is the ideality factor of the diode, thermal leakage voltage is presented as V_{th}, the photocurrent of the module is represented as I_{ph}, the reverse saturation current of the diode is represented as I_0, and the ohmic resistances are represented as R_{se} and R_{sh}. The thermal leakage voltage is equal to N_skT/q, in which the series-connected PV cells are represented as N_s, k is Boltzmann's constant, T is the absolute temperature, and q is the electron charge.

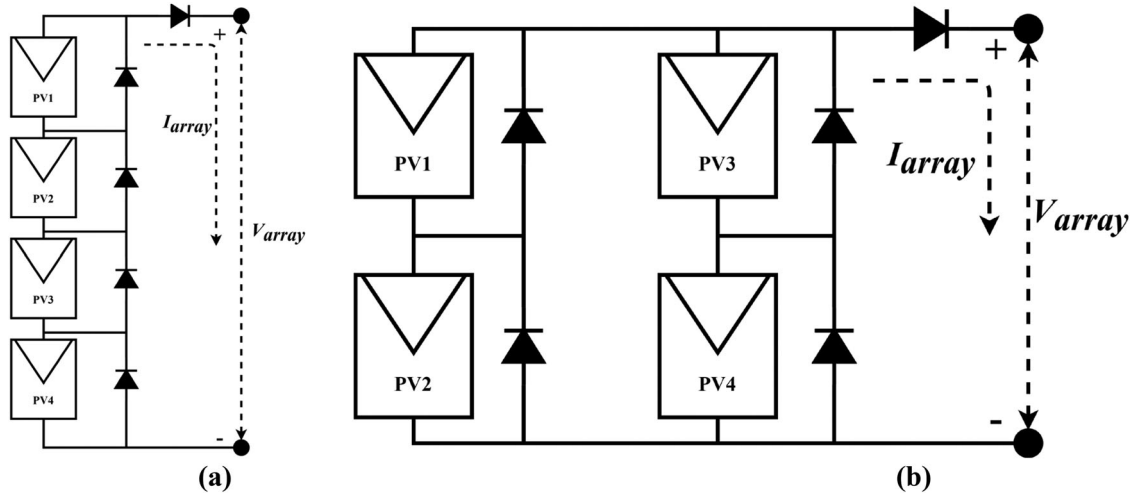

Figure 2. PV array configurations; (a) 4S configuration, (b) 2S2P configuration.

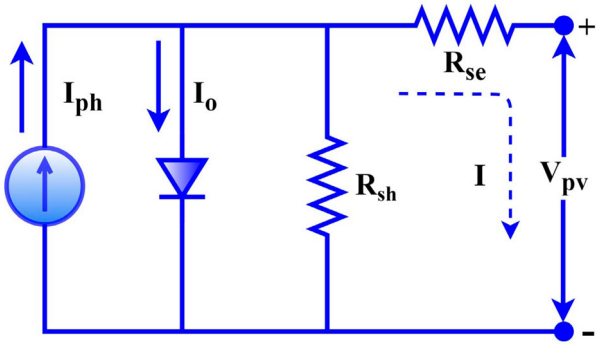

Figure 3. SDM model of the PV cell.

The temperature effects are generally not severely affected, so this paper primarily investigates the irradiance effect on the output properties of a photovoltaic array under PSCs. The PV array output current ($I_{pv,\text{array}}$) comprising parallel strings N_{sh} and series PV modules N_{se} in a string is represented as follows.

$$I_{\text{array}} = I'_{ph} - I'_0\left[exp\left(\frac{V_{\text{array}} + xI_{\text{array}}R_{se}}{nV_{th}{}'}\right) - 1\right] - \left[\frac{V_{\text{array}} + xI_{\text{array}}R_{se}}{xR_{sh}}\right] \quad (2)$$

Where the output current and voltage of the PV array is represented as I_{array} and V_{array}, respectively, x is equal to N_{se}/N_{sh}, I'_0 is equal to $N_{sh}I_o$, I'_{ph} is equal to $N_{sh}I_{ph}$, and V'_{th} is equal to $N_{se}V_{th}$.

2.2. PSCs on the photovoltaic array

The PV array is formed by connecting more number PV modules in series and series/parallel combinations. Due to the change in environmental conditions, the PV cells in the panel are partially shaded. The PV cell subjected to the shading absorbs more energy due to the reverse voltage. The absorbed energy is transformed to the hotspot, and it results in high thermal stress and damages the PV cell junction. The bypass diodes are connected across the cell/panel to reduce the effect due to the hotspot. So, the negative voltage due to the reverse voltage is avoided as per the discussion in [42]. The bypass diode starts its function when the condition given in Equation (3) is satisfied.

$$V_g = \sum_{i=1}^{n} V_i \geq V_D, i \neq 2 \quad (3)$$

The effect on the PV array due to the PSCs is shown in Figure 4, and it is observed that voltage- power characteristic of the PV array exhibits multiple local peak (LP) points during the shading condition and one global peak (GP) point. The most referred PV array configuration, such as 4S (four series-connected panels) and 2S2P (two series-connected panels are connected in parallel), as shown in Figure 2 are considered to validate the performance of the proposed hybrid algorithm. The hybrid algorithm is suitable for other PV array configurations such as honey-comb, total-cross-tied, and bridge-linked. However, for simplification, the testing with the other PV array configurations is not discussed in this paper, which is out of the scope.

The maximum power derived from the panel is formulated as an enlarged problem, and the optimized problem is presented in Equation (4).

$$\text{Maximize the power extraction subjected to } d_{\min} \leq d \leq d_{\max} \quad (4)$$

Where d is the duty cycle of the conventional boost converter, the minimum duty ratio is represented by $d_{\min}$, $d_{\max}$ represents the maximum duty cycle, and the values are restricted as 0.45–0.70, respectively. The maximum duty ratio is fixed at 0.70 to reduce the reverse recovery on the diode and the switching device.

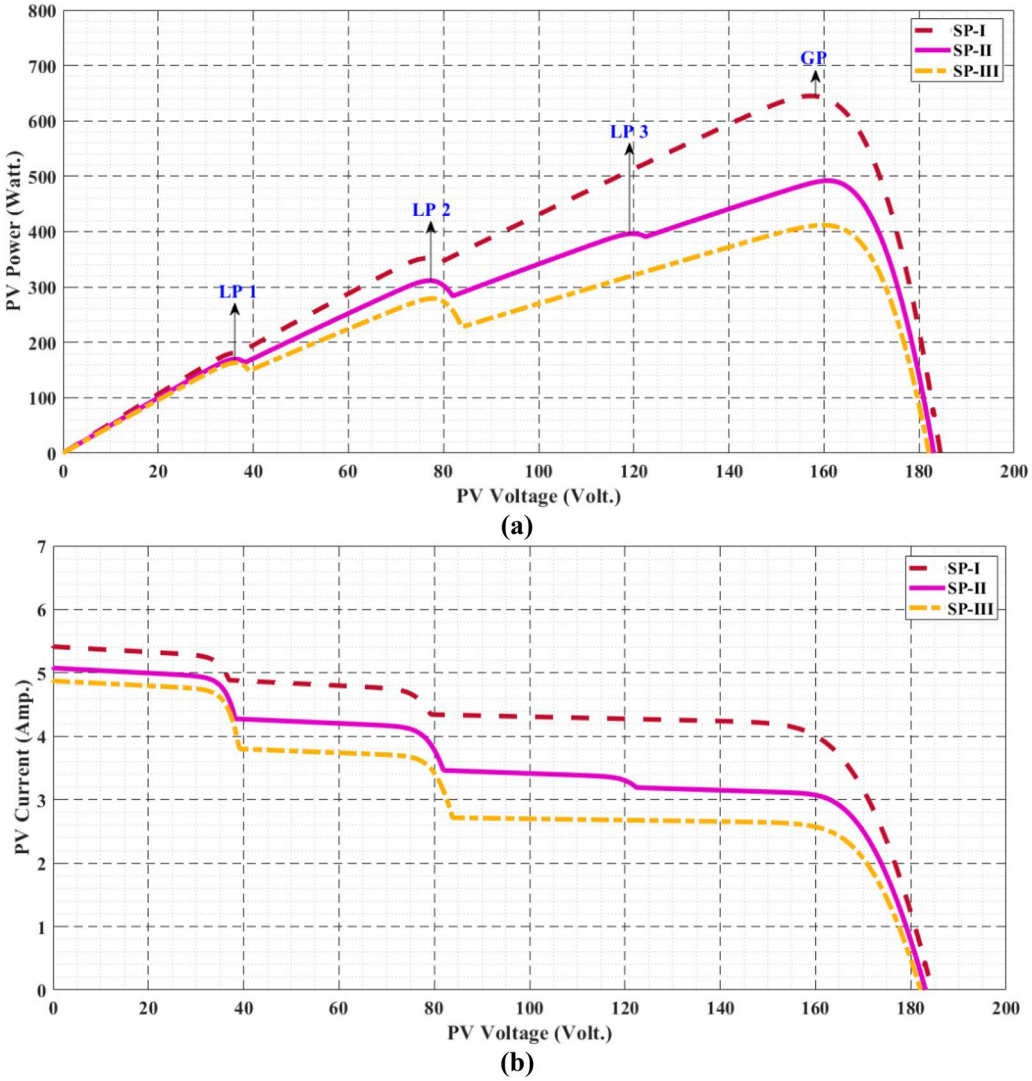

Figure 4. PV array characteristics under different shading patterns; (a) P-V characteristics, (b) I-V characteristics.

3. Hybrid salp swarm optimization algorithm and its application in MPPT

3.1. Basic concepts of salp swarm optimization algorithm

The motivation of this paper is based on the swarm behaviour of salp. The shape of the salp is barrel-shape, and the transparent body and the salp have belonged to the family of Salpidae. Salp tissue looks like a jellyfish, and the movement of salps is also similar to jellyfish. The salps are moving forward by pushing the water through the salp body, and this action resembles propulsion. The shape of the salp is pictured in Figure 5(a). The exciting feature of the salp is the main inspiration of this paper. In the ocean, the salps are grouped into a swarm called salp-chain [43,44], and Figure 5(b) shows the salp-chain formation. The purpose of salp-chain formation is an unknown fact to the researchers, and few researchers believe that the salp-chain is used for a better change in coordination and mobilization using foraging.

3.2. Mathematical modeling of the salp-chain

The authors of [29,45,46] proposed a mathematical model for the salp-chain, and the same can be used for the optimization issues. The population can be grouped into two groups, such as leader and follower. The forward salp is called as a leader, and the leftover salps are called as a follower. The leader salp gives guidance to the follower salp. Like other similar optimization algorithms, the position of the salp in SSA is defined as n-dimensional search space, in which n is a number of variables. The position of the salp is stored in a 2-dimensional search space. The food source in the space is assumed as a swarm target. Equation (5) presents the update for the leader position.

$$P_j^1 = \begin{cases} G_j + c_1((ub_j - lb_j)c_2 + lb_j)c_3 \geq 0 \\ G_j - c_1((ub_j - lb_j)c_2 + lb_j)c_3 < 0 \end{cases} \quad (5)$$

Where P_j^1 is the position of the leader in the j^{th} dimension, G_j is the food source, the lower and upper

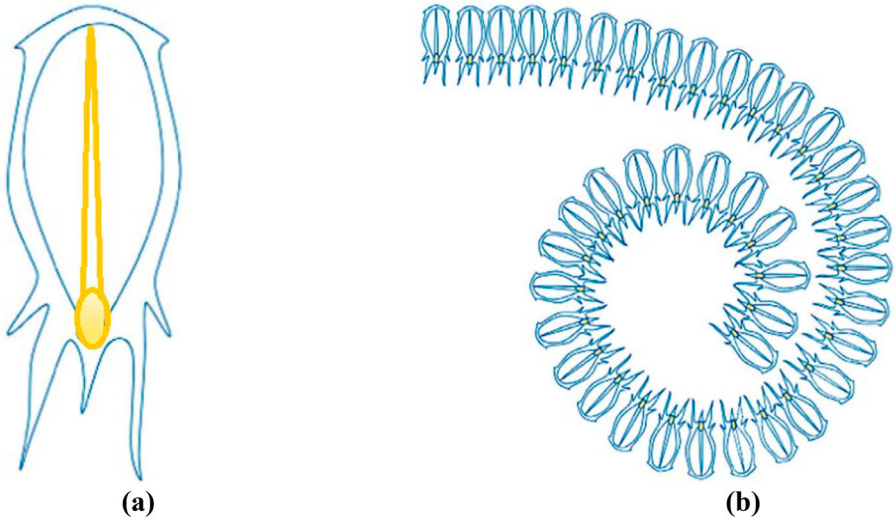

Figure 5. Pictorial representation of salp [25]; (a) Single salp, (b) Salp-chain.

boundary is represented as lb_j and ub_j respectively, c_1, c_2, and c_3 are the random numbers. It is noticed that the leader position is updated about the food source. The random number c_1 is the most significant coefficient in SSA, and it decides the exploration and exploitation. The expression for the c_1 is presented in Equation (6).

$$c_1 = 2e^{-\left(\frac{4l}{L}\right)^2} \tag{6}$$

Where the maximum iteration is represented by L and l represents the current iteration. The other random numbers, such as c_2 and c_3, are selected randomly between [0, 1]. As per Equation (7), the follower position is updated.

$$P_j^i = \frac{1}{2}at^2 + V_o t \tag{7}$$

Where P_j^i is the follower position in the jth dimension, and $i \geq 2$, V_o is the initial speed, $a = V_{\text{final}}/V_o$, and $V_{\text{final}} = x - x_o/t$. Let $V_o = 0$, and "t" is the time in optimization. So, Equation (7) is modified and presented in Equation (8).

$$P_j^i = \frac{1}{2}(P_j^i + P_j^{i-1}) \tag{8}$$

Equations (5–8) is used to model the SSA using the MATLAB/Simulink, and the same has been simulated to check its performance.

3.3. Traditional perturb and observation algorithm

As discussed in [47], before and after each perturbation, the P&O algorithm locates the maximum operating PV voltage by spotting the small change in the PV output power. As per the many researcher's points of view, the conventional P&O algorithm is the most popular and preferable MPPT technique, and it is the base reference to derive and develop a new MPPT technique. The PV output power of the panel is calculated and analysed within the algorithm by providing the sensed PV output voltage and PV output current as input parameters. The algorithm provides the perturbation as per the change in the PV output power processed by the algorithm, and it changes the duty ratio of the converter. The algorithm rule is presented in Equation (9).

$$d_{\text{new}} = \begin{cases} d_{\text{old}} + \varepsilon, if P_{pv} > P_{pv(\text{old})} \\ d_{\text{old}} - \varepsilon, if P_{pv} < P_{pv(\text{old})} \end{cases} \tag{9}$$

Where d_{old} is the old duty ratio, the perturbed duty cycle is represented as ϵ, and d_{new} is the new duty ratio. The fast convergence is achieved by considering large value for ϵ; however, it results in high steady-state oscillation.

3.4. Proposed hybrid SSA-P&O solar PV MPPT technique

The grouping of the salp swarm algorithm and P&O algorithm is called the hybrid SSA-P&O MPPT technique, and it is an advanced computation algorithm for the solar PV system. The P&O algorithm tracks the maximum operating point under uniform irradiance, and the SSA algorithm locates the global peak under non-uniform irradiance conditions. During execution, the SSA algorithm comes into action first, followed by the P&O algorithm. When salps are close to each other, the P&O is in operation at the best salp location in the SSA algorithm process. Figure 6 shows the overall flowchart for the proposed hybrid SSA-P&O algorithm. The main objective of the proposed algorithm is to find the GP under PSCs. In the salp-chain, the follower salp follows the leader salp, and the leader salp moves forward to reach the food source. The food source is replaced by MPP; however, the salp-chain moves near to the MPP. The preeminent solution so far is the maximum power point and the salp-chain moves to the food

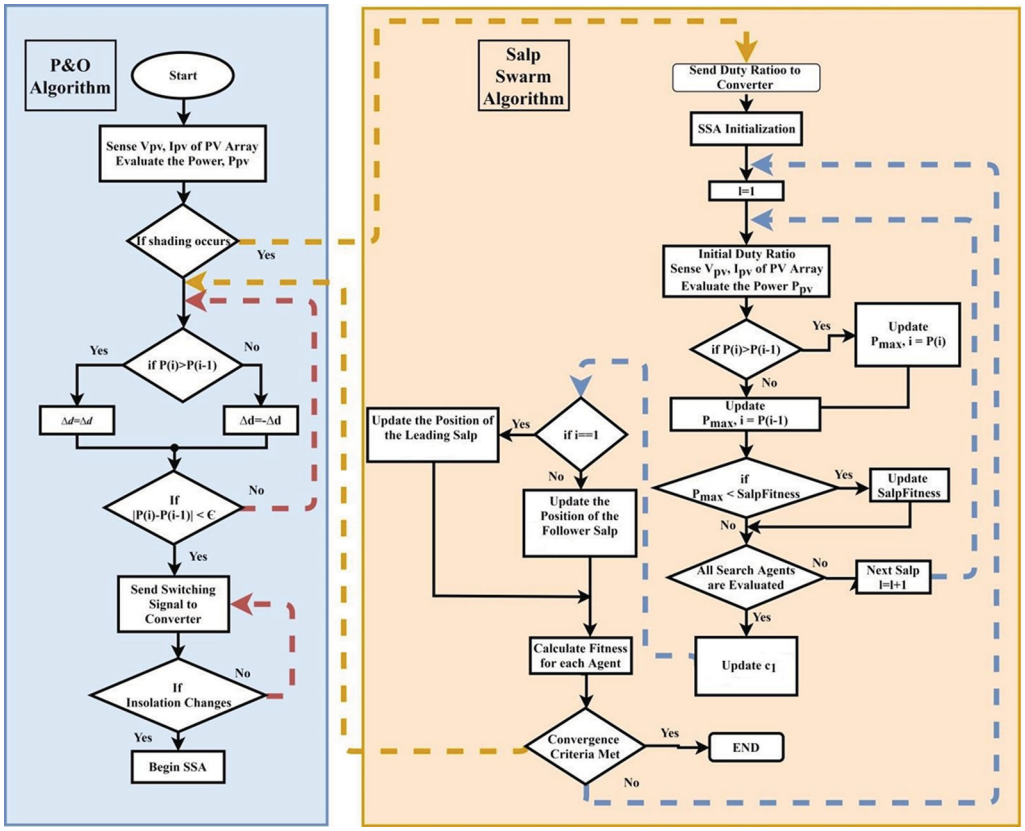

Figure 6. Overall flowchart for the proposed hybrid SSA MPPT technique.

source. Finally, the P&O algorithm locates the GP accurately. The following steps are involved in developing and implementing the proposed hybrid SSA algorithm. The flow of the hybrid SSA technique started with the initial optimum value by allocating the random position for the salps. This approximation finds fitness and determines the greatest fitness salp. The position of the best salp is allocated as a food source. The random c_1 coefficient is keep updated using Equation (10). The leader salp position is to keep updated at each dimension as per Equation (7) and Equation (11) updates the follower salp position.

The salp position is maintained within the search space. The SSA algorithm initially finds the optimal power point under the non-uniform irradiation condition, and finally, P&O converges to GP under normal operating conditions. The salp swarm move near the GP and the position of the leader salp represent the duty cycle for the dc-dc converter which eliminates usage of different controllers and reduces the frequent controller gain tuning, results in the simple control structure. The block diagram of the proposed hybrid SSA MPPT is shown in Figure 7. Depending on the environmental conditions such as solar irradiation and cell temperature, the output PV power is continuously oscillating. The hybrid MPPT algorithm is reinitialized when PV output power changes. By increasing the number of salps, the tracking accuracy is improved; however, a large number of salps increase the computation burden on the algorithm execution. So, the number of salps in the salp-chain is considered as 30 to reduce the computation time in this paper.

4. Results and discussions

The proposed hybrid SSA-P&O algorithm is validated on the different PV configurations by comparing the simulation results acquired by the HGWO, HWOA, and the conventional P&O algorithms. The proposed algorithm is implemented and tested with the conventional boost converter under a change in insolation condition and PSCs. As discussed earlier, there is two PV array configuration considered such as 4S and 2S2P configurations under PSCs for testing the proposed MPPT technique. The PV power generation system is made with PV array, dc-dc boost converter, MPPT controller, and the load for testing. The PV panel specification is given as follows; $V_{mp} = 40$ V, $I_{mp} = 5$ A, $V_{oc} = 47.8$ V, $I_{sc} = 6.2$ A, $P_{mp} = 200$ W, and number of PV cells = 72. The commonly used dc-dc boost converter is designed as per [48], and design parameters of the converter are as follows: $f_s = 100$ kHz, $V_{in} = (24–150$ V), $V_{\text{out}} = 388$ V, $L_{dc} = 1.7$ mH, $C_{\text{out}} = 100$ µF, 450 V (electrolytic), and ripple voltage is assumed as less than 1%. The load resistance is selected as 22 Ω. The proposed algorithm is tested under various shading patterns, and the same is listed in Table 1. The duration for each shading pattern is 0.5 sec, and the computation time is depending upon the various other parameters. To validate

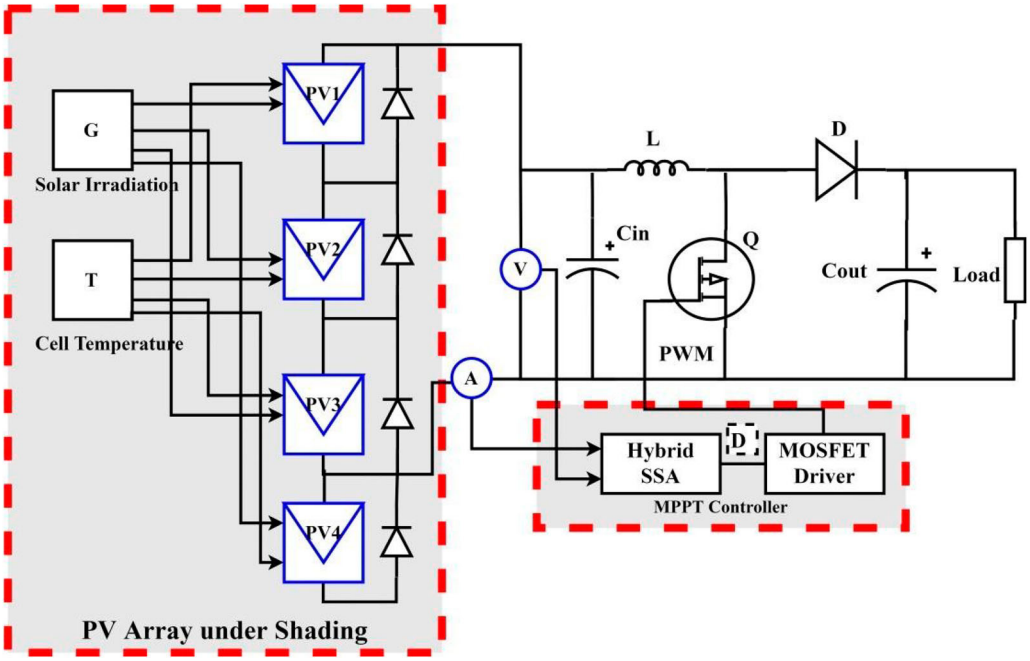

Figure 7. Block diagram of the proposed hybrid MPPT technique.

Table 1. Various shading pattern for the PV array configurations.

Shading Pattern	Pattern 1	Pattern 2	Pattern 3	Pattern 4	Pattern 5	Pattern 6	Pattern 7	Pattern 8
Solar Irradiation (W/m^2)	550	650	850	500	600	700	950	850
Condition	Rapid Change in Insolation						PSCs	
PV Array	4S				2S2P		4S	2S2P
Extreme change in insolation – 200 W/m^2 – 300 W/m^2 – 600 W/m^2 – 900 W/m^2 (for both 4S & 2S2P)								

Table 2. Various parameters of different MPPT techniques.

MPPT Technique	No. of Search Agents	Lower Limit (d_{min})	Upper Limit (d_{max})	Maximum Iterations	No. of Input Variables	No. of Output Variables
HWOA	30	0.45	0.71	10	2 (V_{pv}, I_{pv})	1 (Duty ratio)
HGWO	30	0.45	0.74	10	2 (V_{pv}, I_{pv})	1 (Duty ratio)
HSSA	30	0.45	0.70	10	2 (V_{pv}, I_{pv})	1 (Duty ratio)
P&O	–	0.45	0.92	–	2 (V_{pv}, I_{pv})	1 (Duty ratio)

the performance of the proposed hybrid algorithm, the algorithm parameters are kept constant for all the techniques. The operating parameters are listed in Table 2.

4.1. Simulation results

The simulation of the proposed PV systems is performed using MATLAB/Simulink 2018a using a Laptop with an Intel^R Core (TM) i5-4210U CPU at 2.40 GHz and RAM of 8 GB. The solver in MATLAB is ODE45 (Dormand-Prince), and step size is selected as auto variable-step. The performance of HSSA is compared with the other hybrid metaheuristics algorithms, such as HGWO and HWOA. The maximum number of iterations and population size are significant parameters of the metaheuristic algorithms. Therefore, these two parameters are selected based on various trials and the information from the literature. To have a fair comparison among various algorithms, the parameters are selected as 10 and 30, respectively, as listed in Table 2.

4.1.1. Performance of the solar PV array under a dynamic change in insolation

The solar PV array's output power, voltage, and current waveforms for 4S array configuration under a dynamic change in insolation for the proposed hybrid technique and other techniques, such as HGWO, HWOA, and P&O, are presented in Figure 8. Figure 8 shows the PV power output along with the PV output voltage and the current for a better understanding of the readers. However, in the text, PV output tracking power has been presented for each of the shading patterns. As per Table 1, three shading patterns are created to validate the performance of the algorithm. The pattern-1 is generated at 0.5 sec, pattern-2 is generated at 1 sec, and pattern-3 is generated at 1.5 sec. During the pattern-1, the proposed hybrid HSSA MPPT technique converges to GP at 688.6 W, the HWOA locates the GP

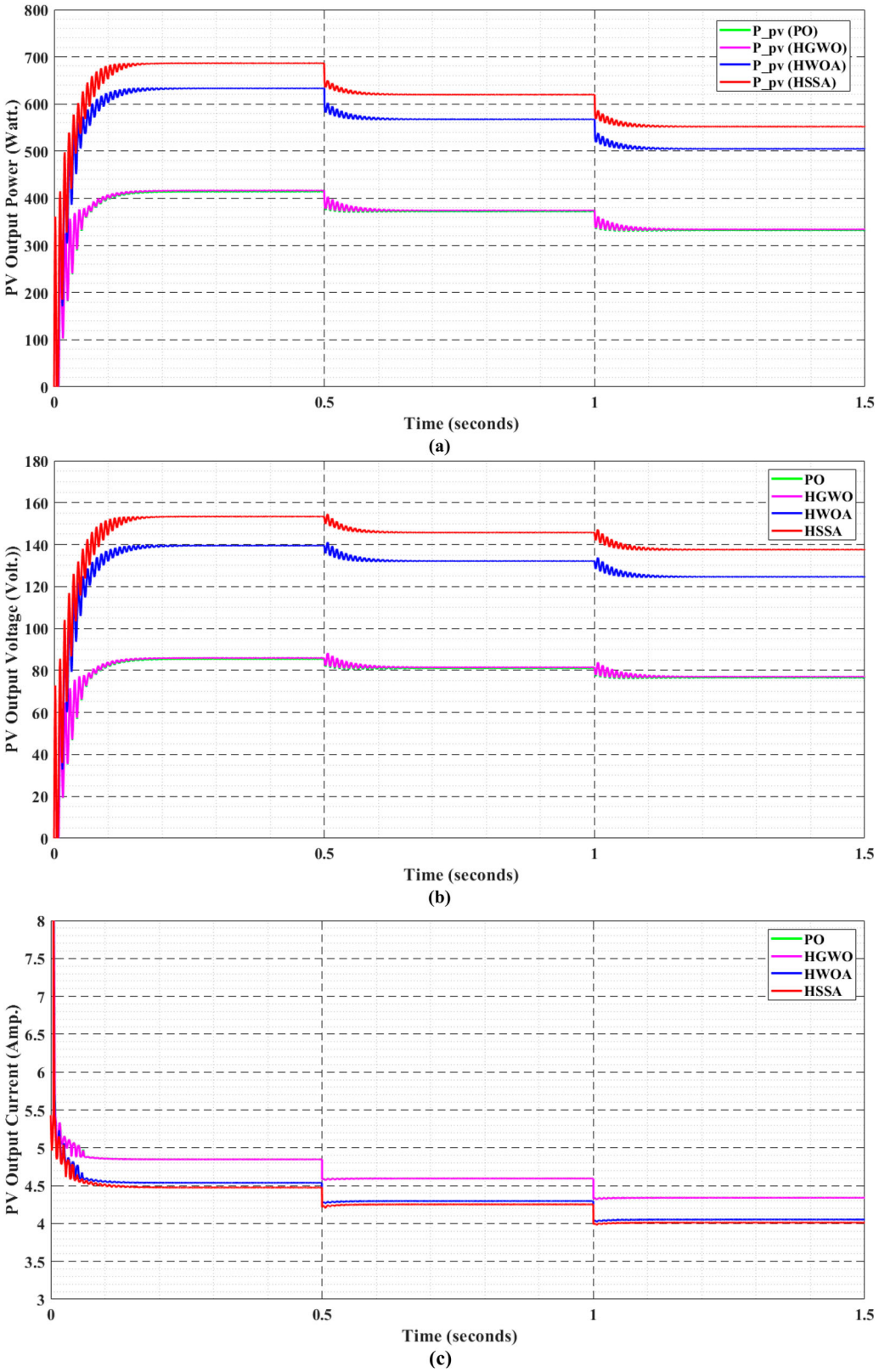

Figure 8. 4S PV array configuration under a dynamic change in insolation; (a) PV output power in watts., (b) PV output voltage (Volts.), (c) PV output current (Amps.).

at 631.2 W, the HGWO locates at 413.5 W, and the P&O tracks the GP at 411.1 W. The pattern-2 is switched from the shading pattern-1 at 1 sec. During the pattern-2, the HSSA technique converges to GP at 628.1 W, the HWOA tracks the GP at 575.7 W, HGWO converge to GP at 389.2 W, and the P&O tracks the GP at 384.6 W. The pattern-2 is changed to pattern-3 at 1.5 sec. During the shading pattern-3, the HSSA technique converges to GP at 575.1 W, the HWOA tracks the GP at 501.4 W, the HGWO locates the GP at 332.4 W, and the PO tracks the GP at 331.1 W. It is observed from the Figure 9 that the P&O and HGWO algorithm fails to track the GP, and it

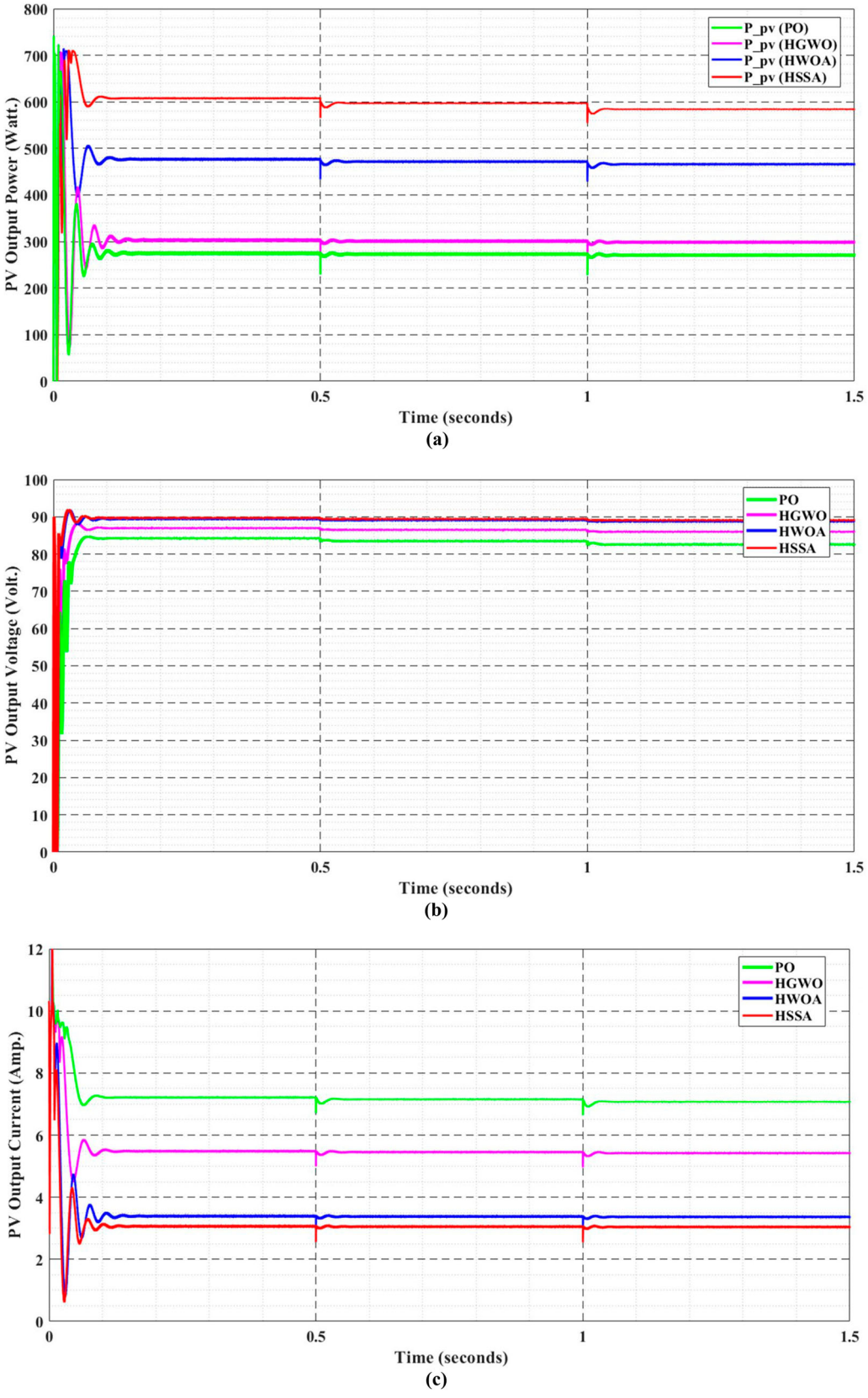

Figure 9. 2S2P PV array configuration under a dynamic change in insolation; (a) PV output power in watts., (b) PV output voltage (Volts.), (c) PV output current (Amps.).

is concluded that the proposed hybrid HSSA algorithm displays a higher tracking speed with accuracy, and the power oscillation is less compared to other techniques.

Figure 9 shows the PV output power along with the PV output voltage and the current for 2S2P PV array configuration. Similar to the 4S configuration, three shading patterns are created. During the pattern-4, the proposed hybrid HSSA MPPT technique converges to GP at 610.2 W, the HWOA locates the GP at 478.1 W, the HGWO locates at 304.5 W, and the P&O tracks the

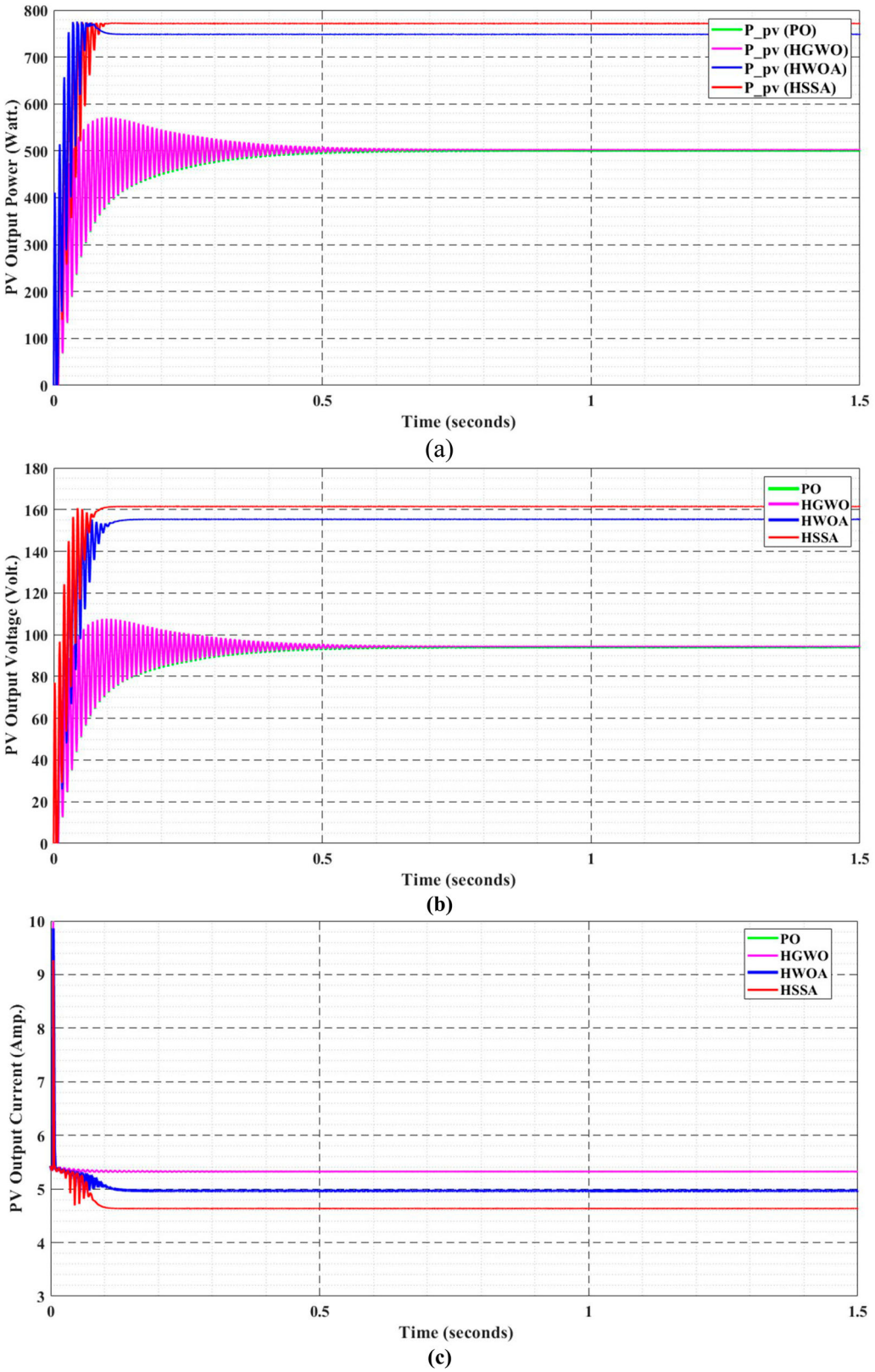

Figure 10. 4S PV array configuration under PSCs; (a) PV output power in watts., (b) PV output voltage (Volts.), (c) PV output current (Amps.).

GP at 279.4 W. During the pattern-5, the HSSA technique converges to GP at 598.2 W, the HWOA tracks the GP at 475.2 W, HGWO converge to GP at 299.5 W, and the P&O tracks the GP at 278.1 W. During the shading pattern-6, the HSSA technique converges to GP at 588.2 W, the HWOA tracks the GP at 469.9 W, the HGWO locates the GP at 298.7 W, and the PO tracks the GP at 276.4 W. It is observed from the Figure 10 that the P&O, HGWO, and HWOA algorithm fails to track the GP, and it is concluded that the proposed algorithm displays a higher tracking speed, and the power oscillation is less.

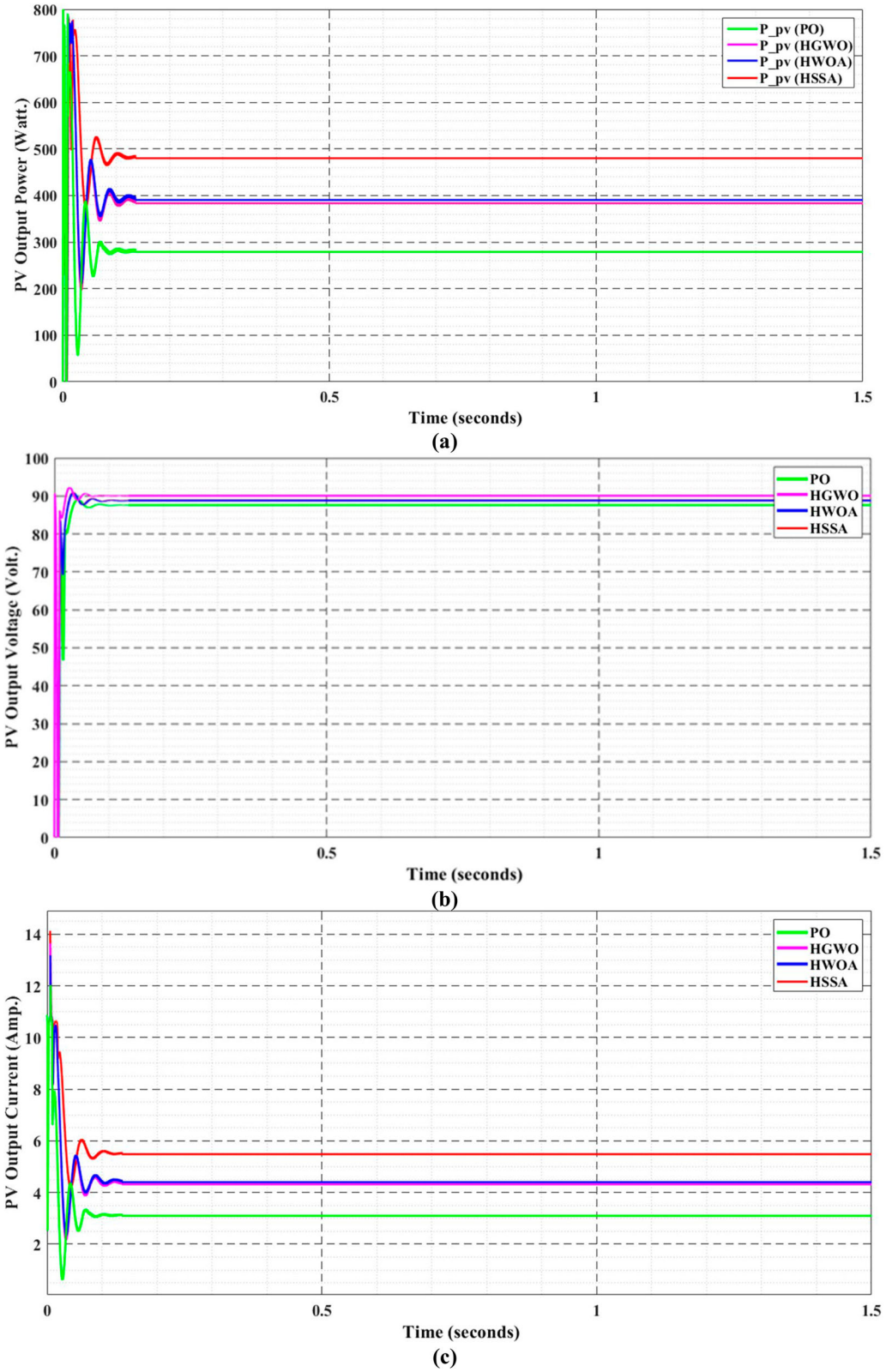

Figure 11. 2S2P PV array configuration under PSCs; (a) PV output power in watts., (b) PV output voltage (Volts.), (c) PV output current (Amps.).

4.1.2. Performance of the solar PV array under PSCs

Similar to subsection 4.1, the PV power system is simulated for 4S configuration under PSC at the pattern-7, and the respective waveforms are presented in Figure 10, and the same is extended for 2S2P PV array configuration at the pattern-8, and the respective waveforms are presented in Figure 11. From Figure 10–11, it is noticed that the hybrid HSSA-P&O MPPT technique converges fast to GP as compared with the conventional PO, HWOA, and HGWO techniques. The proposed hybrid MPPT technique tracks/extracts the high output power from the solar PV array. However, the HGWO and P&O algorithm track significantly less PV output power than the HWOA and HSSA.

The conventional P&O algorithm tracks very less power during the 2S2P PV array configuration than the 4S configuration. So, the P&O algorithm is not suitable for a PV system with PSCs. It is observed that both the HSSA and HWOA converge to GP at a fast rate; however, the HSSA technique extracts roughly around 100 W more than the HWOA with high accuracy for the two PV array configurations.

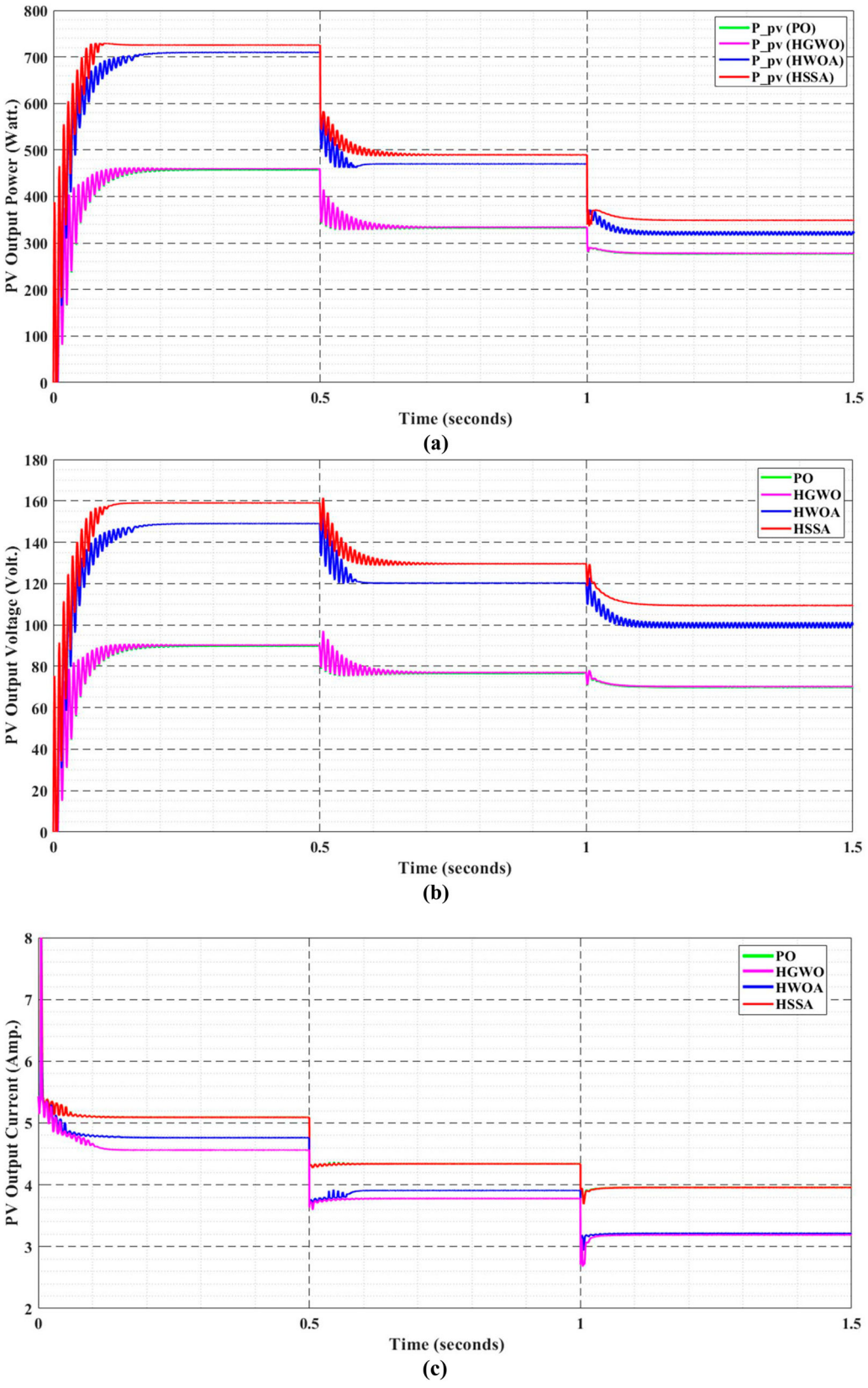

Figure 12. 4S PV array configuration under Extreme change in insolation; (a) PV output power in watts., (b) PV output voltage (Volts.), (c) PV output current (Amps.).

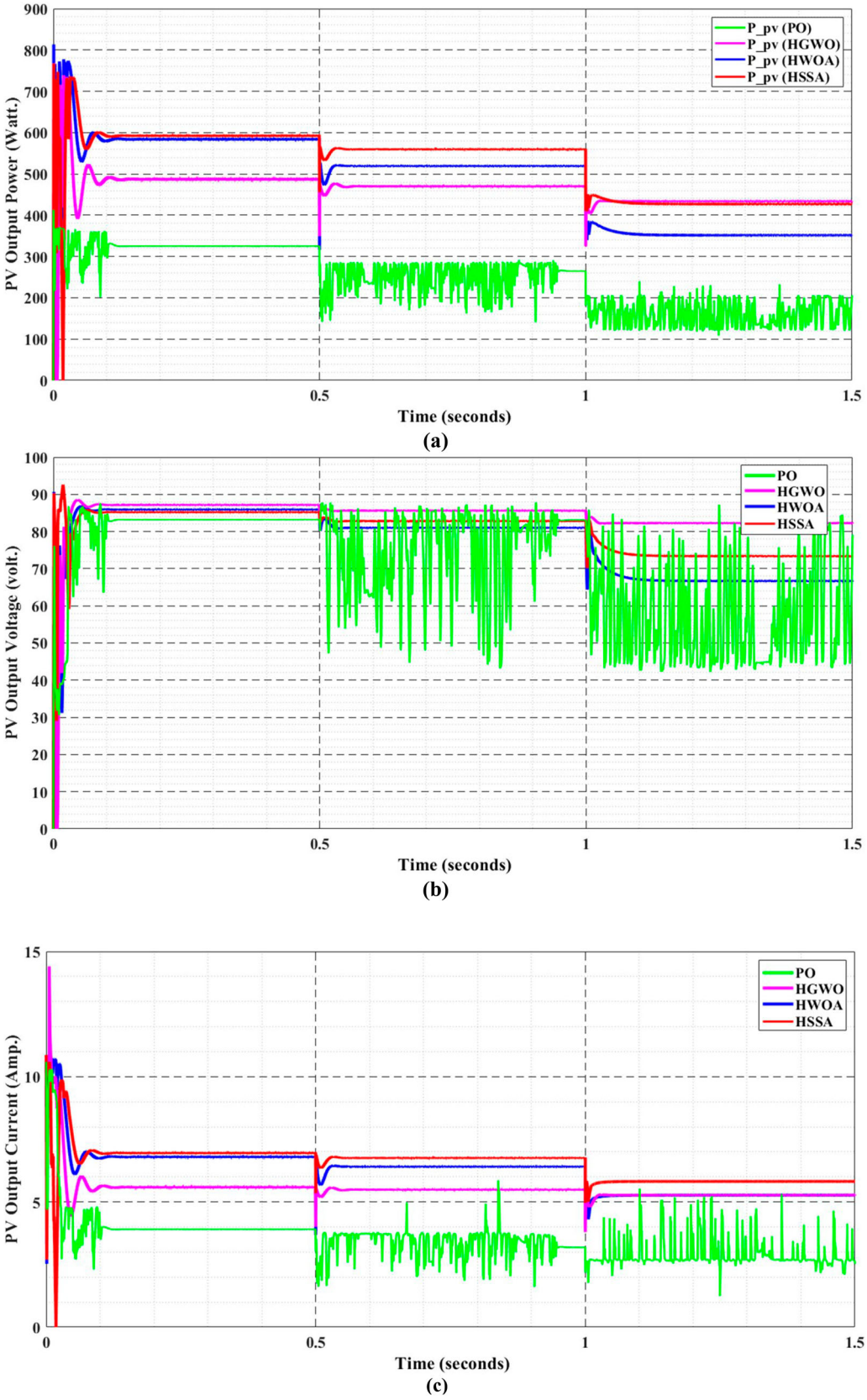

Figure 13. 2S2P PV array configuration under Extreme change in insolation; (a) PV output power in watts., (b) PV output voltage (Volts.), (c) PV output current (Amps.).

4.1.3. Performance of the solar PV array under an extreme change in insolation

The proposed hybrid HSSA is simulated under an extreme change in solar insolation to validate the performance of the proposed algorithm. The output waveforms are shown in Figure 12 for the 4S PV array configuration, and Figure 13 shows the output waveforms for the 2S2P PV array configuration. As similar to previous test conditions, the shading patterns are created at every 0.5 sec. From Figure 12, it is

Figure 14. Experimental setup of the photovoltaic system.

observed that the proposed algorithm converges to GP at 730.8 W during 0–0.5 sec, 494.2 W during 0.5–1 sec, and 362.8 W during 1–1.5 sec.

At the same time, the HWOA technique tracks less power (approximately 24 W) than the proposed technique with almost the same convergence speed. However, the other two techniques, such as HGWO and P&O algorithm, fails to trace the GP under an extreme change in insolation. During an extreme change in insolation, all the MPPT techniques introduce the power oscillation, but the oscillation introduced by HSSA is less with high convergence speed and tracking efficiency. From Figure 13, it is noticed that the P&O algorithm exhibits more power oscillation than the other algorithm due to the inability to track the power under an extreme change in insolation, and it requires frequent tuning on the MPPT controller. The proposed algorithm and the HWOA exhibit the same operating performance; however, the proposed hybrid algorithm converges to GP at a fast rate with high tracking efficiency. The HGWO algorithm takes more time to converge to GP with less tracking efficiency due to the restriction in the upper and lower limit of the duty ratio of the dc-dc converter.

4.2. Experimental results

The simulation and theoretical discussions are validated through real-time experimentation. Therefore, the experimental prototype is made for laboratory testing, and the same is depicted in Figure 14. As similar to the simulation study, the proposed HSSA is validated for two PV array configurations, such as 4S and 2S2P PV array configurations. The shading pattern on the PV modules is artificially created is created. The DSpace 1103 development board process the input signals and generates the PWM pulse to control the switching operation of the boost converter. The sensors, such as LA25-NP and LV25-P, are used to sense the PV array current and PV array voltage, respectively. The raw signals are processed by the signal conditioning units and sent to the DSpace 1103, which further processes the signals and generates the gate pulse with the required duty cycle.

The performance of the HSSA is validated for two different shading patterns. The voltage, current, and current waveforms are captured using control desk NG 5.2. The DSpace and MATLAB/Simulink process the control signals and it sends the PWM pulse to the MOSFET switch of the boost converter. The effectiveness of the proposed HSSA is compared with other hybrid algorithms, such as HWOA and HGWO, since the P&O algorithm fails to track the global peak during a rapid change in insolation conditions. And the same has been proved through the simulation results. The PV array voltage, current, and power waveforms for the 3S configuration are depicted in Figure 15. The shading pattern is changed every 10 sec. intervals. At the initial stage, the proposed HSSA tracks the global peak at 561 W, HGWO converges to 492 W, and HWOA converges to 521 W, as illustrated in Figure 15. As seen in Figure 15(c), the proposed HSSA tracks the GP quickly than the other two hybrid algorithms. The shading pattern is artificially changed at 20 sec., and the proposed HSSA starts to search the global peak throughout the search space. Due to its high exploration and exploitation ability, the HSSA tracks the GP at 529 W, HGWO converges to 418 W, and HWOA converges to 498 W, as illustrated, and at 30 sec., the shading pattern is again changed. The HSSA tracks the GP at 469 W,

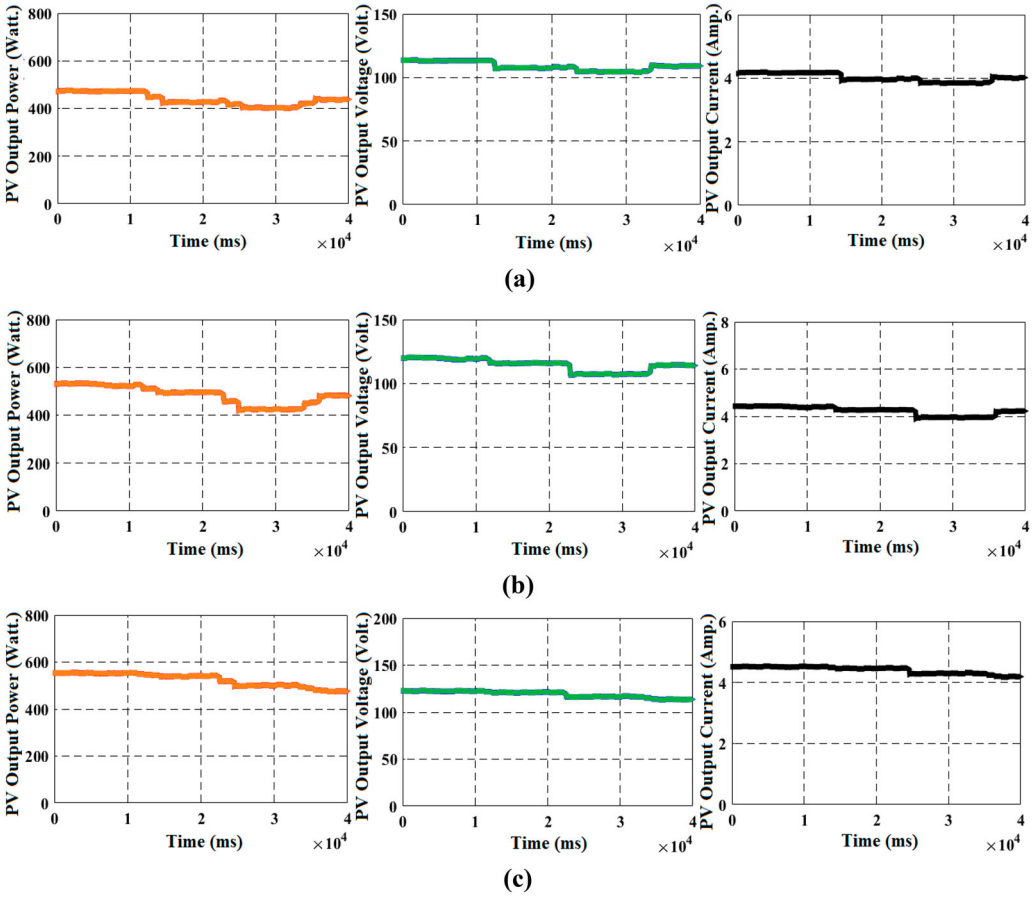

Figure 15. Experimental waveforms for the 3S configuration; (a) HWOA, (b) HGWO, (c) HSSA.

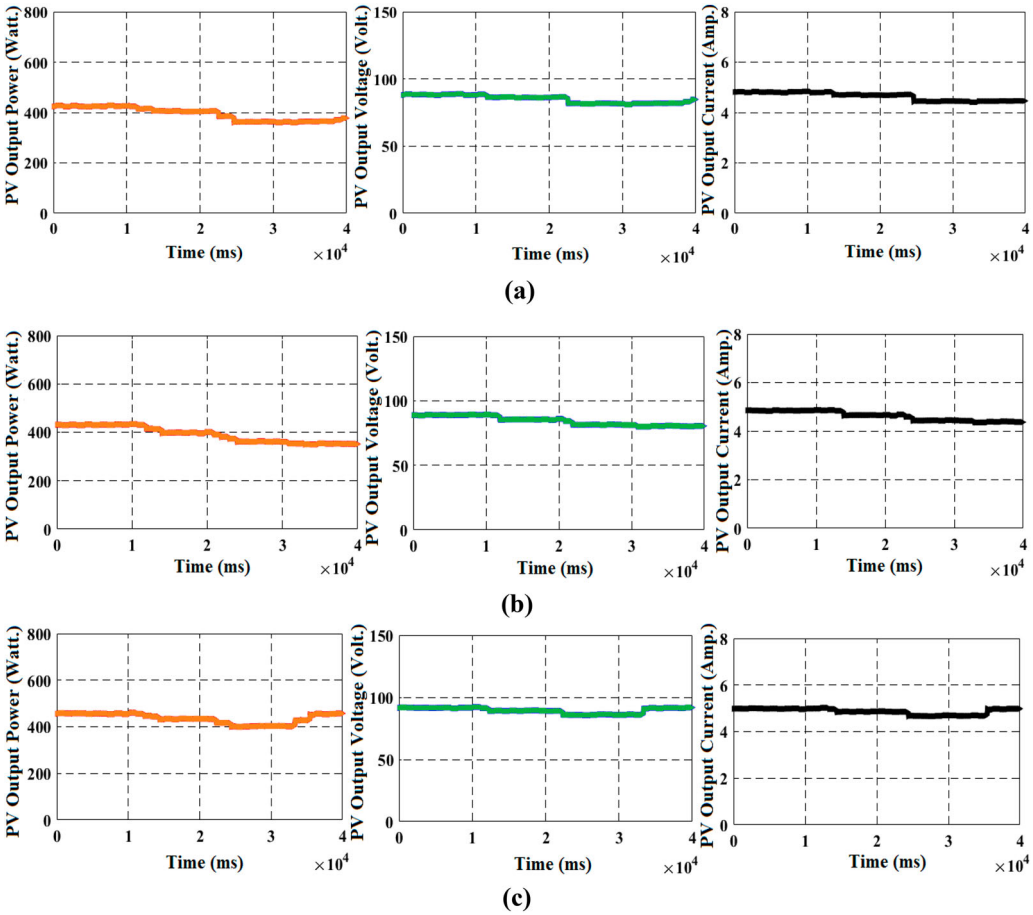

Figure 16. Experimental waveforms for the 2S2P configuration; (a) HWOA, (b) HGWO, (c) HSSA.

Table 3. Comparison of HSSA, HWOA, HGWO and PO MPPT methods.

PV Array	Shading Pattern	MPPT Techniques	PV Power (W)	Tracking Time (Seconds)	P_{max} from the Curve (W)	Efficiency (%)
4S	I	**HSSA**	**688.6**	**0.2145**	**698**	**98.65**
		HWOA	631.2	0.2987	90.42	
		HGWO	413.5	0.3541	59.24	
		PO	411.5	0.3877	58.95	
	II	**HSSA**	**628.1**	**0.2045**	**682**	**92.09**
		HWOA	575.7	0.2987	84.41	
		HGWO	389.2	0.3124	57.06	
		PO	384.6	0.3289	56.33	
	III	**HSSA**	**575.1**	**0.2258**	**600**	**95.85**
		HWOA	501.4	0.2874	83.56	
		HGWO	332.4	0.3035	55.40	
		PO	331.1	0.3365	55.18	
2S2P	IV	**HSSA**	**610.2**	**0.1156**	**676**	**90.26**
		HWOA	478.1	0.1789	70.72	
		HGWO	304.5	0.2251	45.04	
		PO	279.4	0.2785	41.33	
	V	**HSSA**	**598.2**	**0.1457**	**650**	**92.03**
		HWOA	475.2	0.1976	73.17	
		HGWO	299.5	0.2399	46.07	
		PO	278.1	0.2874	42.78	
	VI	**HSSA**	**588.2**	**0.1754**	**620**	**94.87**
		HWOA	469.9	0.1937	75.79	
		HGWO	298.7	0.2547	48.17	
		PO	276.4	0.2691	44.58	

The bold letter indicates the best results.

Table 4. Comparative analysis of various MPPT techniques.

MPPT Methods	Regular Tuning	Response	Power Oscillation	GP Convergence	Execution Time	Difficulty
HSSA	No	Very quick and accurate	Very Less	Guaranteed	0.0032* 0.0042** 0.0054***	Medium
HWOA	No	Quick and less accuracy	Less	Guaranteed	0.0058* 0.0092** 0.0112***	Medium
HGWO	No	Moderate and poor accuracy	Moderate	Guaranteed	0.0101* 0.0158** 0.0458***	Medium
PO with a step size of 0.05	Yes	Sluggish and poor accuracy	Very High	Not Guaranteed	0.0028* 0.0034** 0.0042***	Easy

*Start-up, **PSCs, and ***Rapid insolation change.

HGWO converges to 409 W, and HWOA converges to 406 W.

Similar to the above study, the performance of the 2S2P configuration is validated for different shading conditions. The PV array voltage, current, and power waveforms for the 2S2P configuration is depicted in Figure 16. The shading pattern is changed every 10 sec. intervals. At the initial stage, the proposed HSSA tracks the global peak at 445 W, HGWO converges to 405 W, and HWOA converges to 395 W, as illustrated in Figure 16. As seen in Figure 16(c), the proposed HSSA tracks the GP quickly than the other two hybrid algorithms. The shading pattern is artificially changed at 20 sec., and the proposed HSSA starts to search the global peak throughout the search space. Due to its high exploration and exploitation ability, the HSSA tracks the GP at 422 W, HGWO converges to 404 W, and HWOA converges to 401 W, as illustrated, and at 30 sec., the shading pattern is again changed. The HSSA tracks the GP at 421 W, HGWO converges to 375 W, and HWOA converges to 368 W.

From Figure 15–16, it is noticed that the HSSA locates the GP precisely under a change in solar insolation conditions. The HSSA also results in a high tracking efficiency with a quicker convergence. From the above all the discussions, it has been decided that the proposed hybrid HSSA MPPT technique can able to work in all the operating conditions such as PSCs, fast change in insolation, and an extreme change in insolation. The performance of the proposed hybrid HSSA, HWOA, HGWO, and P&O techniques are compared with regard to the tracking speed and tracking efficiency, and the same is listed in Table 3. The operating features of the algorithms discussed in the paper are presented in Table 4. The performance characteristics of the different PV array configurations with the various MPPT techniques are shown in Figures 17–18. The tracking speed of all the techniques is presented in Figure 17 and Figure 18 shows the tracking efficiency of all the MPPT techniques.

The proposed hybrid HSSA MPPT technique results in high convergence speed with very high tracking

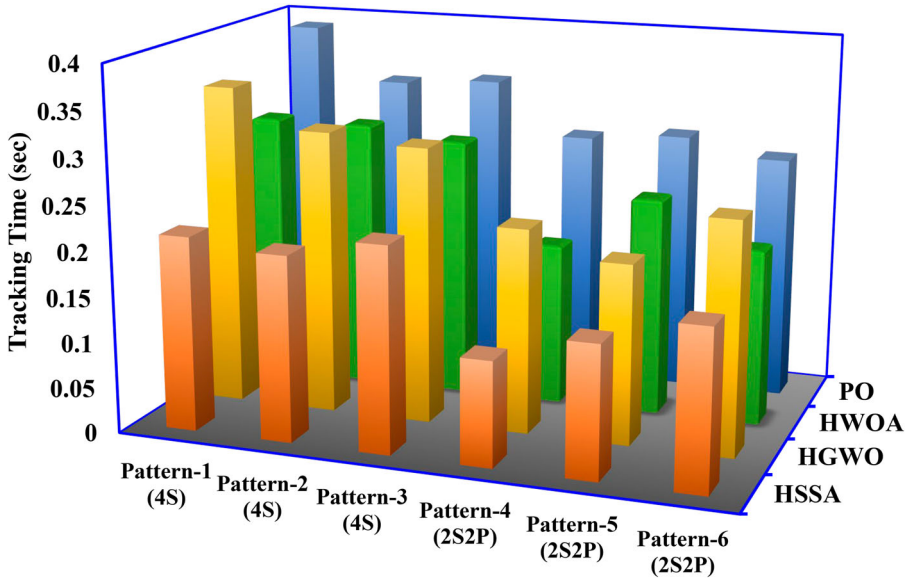

Figure 17. Tracking speed of all MPPT methods.

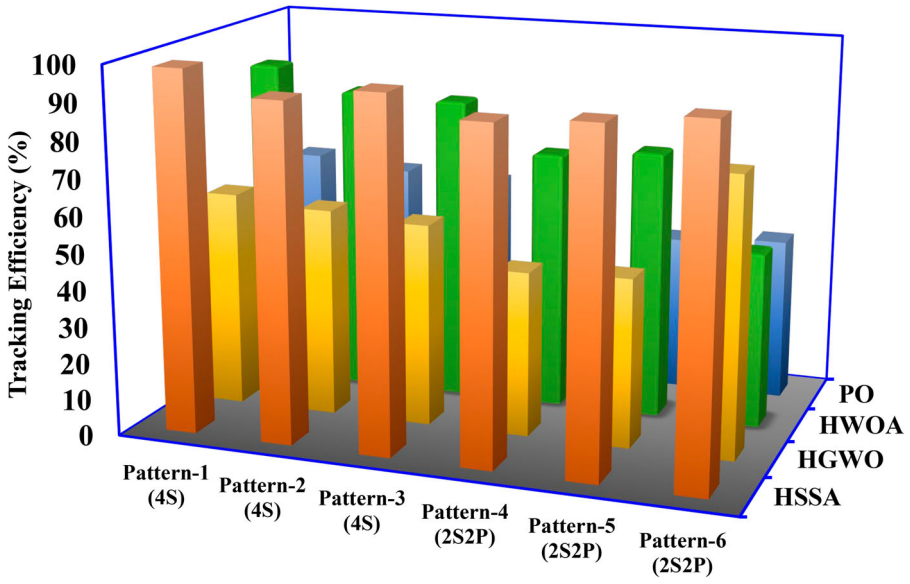

Figure 18. Tracking efficiency of all MPPT methods.

efficiency of the controller. Finally, it is concluded that the proposed HSSA MPPT technique can able to regulate itself towards the extreme change in insolation, fast change in insolation, and PSCs.

5. Conclusions

A novel hybrid HSSA MPPT technique is discussed in this paper to track/locate the GP when the PV based power generation system is subjected to change in shading conditions. The proposed hybrid technique is tested in the laboratory for two various PV array configurations under different operating conditions such as PSCs, fast change in insolation, and extreme change in insolation. When the PV based power generation system exhibits multiple LPs, the proposed technique can able to locate the GP accurately with fast-tracking speed and high tracking efficiency for all the test conditions. From the test results and the discussions, the proposed hybrid MPPT technique is more significant in tracking speed, accuracy, and efficiency. The computation burden of the HSSA technique is reduced by less search agents. In this paper, the 30 number of search agents are selected with 10 iterations for the HSSA technique. From the results, it is noticed that the proposed method has a low standard deviation, which allows the HSSA technique to locate the GP efficiently. The ability of the proposed algorithm is proved by the laboratory simulation results in both steady-state and transient conditions. In summary, the main contribution/novelty of this paper as follows.

(1) A new hybrid HSSA combined with the conventional P&O is developed, which tracks the MPP during PSCs.

(2) The significant effects of the PSC are analysed and validated through simulation and experimentation.
(3) The standalone meta-heuristic algorithms are implemented with a single search mechanism. The proposed HSSA can use multiple searches using the basic SSA during steady-state and P&O during the transient state, which helps to generate more energy.

In the future, the proposed HSSA will be implemented using a low-cost microcontroller board called Arduino for a low rating photovoltaic system. The proposed HSSA MPPT will also be tested by considering the inverter for a real-time system.

Disclosure statement

No potential conflict of interest was reported by the author(s).

ORCID

M. Premkumar http://orcid.org/0000-0003-1032-4634
C. Kumar http://orcid.org/0000-0002-1132-4794
R. Sowmya http://orcid.org/0000-0002-0967-7718
J. Pradeep http://orcid.org/0000-0001-6944-4775

References

[1] Zhengming Z, Libo W, Jianzheng L. A single-stage three-phase grid-connected photovoltaic system with modified MPPT method and reactive power compensation. IEEE Trans Energy Convers. 2007;22(4):881–886.
[2] Bizon N. Global Maximum Power Point Tracking (GMPPT) of photovoltaic array using the Extremum Seeking Control (ESC): a review and a new GMPPT ESC scheme. Renewable Sustainable Energy Rev. 2016; 57:524–539.
[3] Kheldoun A, Bradai R, Boukenoui R, et al. A new golden section method based maximum power point tracking algorithm for photovoltaic systems. Energy Convers Manage. 2016;111:125–136.
[4] Sundareswaran K, Peddapati S, Palani S. Application of random search method for maximum power point tracking in partially shaded photovoltaic systems. IET Renew Power Gener. 2014;14(8):670–678.
[5] Amir A, Selvaraj J, Rahim N. Study of the MPP tracking algorithms: Focusing the numerical method techniques. Renewable Sustainable Energy Rev. 2016;62:350–371.
[6] Abdul-Kalaam R, Muyeen S, Al-Durra A. Review of maximum power point tracking techniques for photovoltaic system. Global J Control Eng Technol. 2016;2:8–18.
[7] Chapman P, Esram T. Comparison of photovoltaic array maximum power point tracking techniques. IEEE Trans Energy Convers. 2007;22(2):439–449.
[8] Saied M, Ali A, Mostafa M, et al. A survey of maximum PPT techniques of PV systems. in Proc of IEEE Energytech. 2012. p. 1–10.
[9] Kerekes T, Sera D, Teodorescu R, et al. Improved MPPT algorithms for rapidly changing environmental conditions. in Proc. of Power Electron Motion Control Conf. 2006; p. 1614–1619.
[10] Narsingoju K, Busa V, Kumar GV. Simulation analysis of maximum power control of photovoltaic power system. Int J Adv Electr Electron Eng. 2012;1(1): 9–14.
[11] Premkumar M, Sowmya R. Certain study on MPPT algorithms to track the global MPP under partial shading on solar PV module/array. Int J Comput Digital Syst. 2019;8(4):405–416.
[12] Premkumar M, et al. Improved perturb & observation maximum power point tracking technique for solar photovoltaic power generation systems. IEEE Syst J. 2020. doi:10.1109/JSYST.2020.3003255.
[13] Premkumar M, Sudhakar Babu T, Sowmya R. Modified perturb & Observe maximum power point technique for solar photovoltaic systems. Int J Sci Technol Res. 2020;9(3):5117–5122.
[14] Gupta N, Patel N, Ladha R, et al. A novel autoscaling variable perturbation size maximum power point tracker applied to photovoltaic (PV) system. Int Trans Electr Energy Sys. 2020;30(3):e12198.
[15] Kjaer SB. Evaluation of the "hill-climbing" and the "incremental conductance" maximum power point trackers for photovoltaic power systems. IEEE Trans Energy Convers. 2012;27(4):922–929.
[16] Yang B, Yu T, Zhang X, et al. Dynamic leader based collective intelligence for maximum power point tracking of PV systems affected by partial shading condition. Energy Convers Manage. 2019;179:286–303.
[17] Sakib N, Kabir M, Rahman MS, et al. A comparative study of flower pollination algorithm and bat algorithm on continuous optimization problems. Int J Appl Inf Syst. 2014;7(9):20–19.
[18] Li H, Yang D, Su W, et al. An overall distribution particle swarm optimization MPPT algorithm for photovoltaic system under partial shading. IEEE Trans Ind Electron. 2018;66(1):265–275.
[19] Mohanty S, Subudhi B, Ray PK. A new MPPT design using grey wolf optimization technique for photovoltaic system under partial shading conditions. IEEE Trans Sustainable Energy. 2016;7(1):181–188.
[20] Kumar C, Rao R. A novel global MPP tracking of a photovoltaic system based on whale optimization algorithm. Int J Renew Energy Dev. 2016;5(03):225–232.
[21] Mansoor M, Feroz Mirza A, Ling Q. Harris hawk optimization-based MPPT control for PV systems under partial shading conditions. J Clean Prod. 2020; 274:122857.
[22] Li S, Chen H, Wang M, et al. Slime mould algorithm: A new method for stochastic optimization. Future Gener Comput Syst. 2020;111:300–323.
[23] Yousri D, Babu TS, Beshr E, et al. A robust strategy based on marine predators algorithm for large scale photovoltaic array reconfiguration to mitigate the partial shading effect on the performance of PV system. IEEE Access. 2020;8:112407–112426.
[24] Yang B, Zhong L, Zhang X, et al. Novel bio-inspired memetic salp swarm algorithm and application to MPPT for PV systems considering partial shading condition. J Clean Prod. 2019;215:1203–1222.
[25] Mohanty S, Subudhi B, Ray PK. A grey wolf-assisted perturb & observe MPPT algorithm for a PV system. IEEE Trans Energy Convers. 2017;32(1):340–347.
[26] El-Helw HM, Magdy A, Marei MI. A hybrid maximum power point tracking technique for partially shaded photovoltaic arrays. IEEE Access. 2017;5:11900–11908.

[27] Premkumar M, Sumithira TR. Humpback whale assis ted hybrid maximum power point tracking algorithm for partially shaded solar photovoltaic systems. Journal of Power Electronics. 2018;18(6):1498–1511.
[28] Doostabad HH, Keypour R, Khalghani MR, et al. A new approach in MPPT for photovoltaic array based on extremum seeking control under uniform and non-uniform irradiances. Sol Energy. 2013;94:28–36.
[29] Mirjalili S, Gandomi AH, Mirjalili SZ, et al. Salp swarm algorithm: a bio-inspired optimizer for engineering design problems. Adv Eng Softw. 2017;114:163–191.
[30] Yıldız BS, Yıldız AR. The harris Hawks optimization algorithm, salp swarm algorithm, grasshopper optimization algorithm and dragonfly algorithm for structural design optimization of vehicle components. Mater Test. 2019;61:744–748.
[31] Premkumar M, Ibrahim AM, Mohan Kumar R, et al. Analysis and simulation of bio-inspired Intelligent salp swarm MPPT method for the PV systems under partial shaded conditions. Int J Comput Digital Syst. 2020;8(5):489–496.
[32] Abbassi R, Abbassi A, Heidari AA, et al. An efficient salp swarm-inspired algorithm for parameters identification of photovoltaic cell models. Energy Convers Manage. 2019;179:362–372.
[33] Qais MH, Hasanien HM, Alghuwainem S. Enhanced salp swarm algorithm: application to variable speed wind generators. Eng Appl Artif Intelli. 2019;80:82–96.
[34] Singh N, Chiclana F, Magnot JP. A new fusion of salp swarm with sine cosine for optimization of non-linear functions. Eng Comput. 2020;36:185–212.
[35] Rizk-Allah RM, Hassanien AE, Elhoseny M, et al. A new binary salp swarm algorithm: development and application for optimization tasks. Neural Computing and Applications. 2019;31:1641–1663.
[36] Kaur S, Awasthi LK, Sangal A. HMOSHSSA: A hybrid meta-heuristic approach for solving constrained optimization problems. Eng Comput. 2020. doi:10.1007/s00366-020-00989-x.
[37] Mirjalili S, Hashim SZM, Sardroudi HM. Training feed-forward neural networks using hybrid particle swarm optimization and gravitational search algorithm. Appl Math Comput. 2012;218:11125–11137.
[38] Bairathi D, Gopalani D. Opposition based salp swarm algorithm for numerical optimization, in: Proc. of the International conference on intelligent systems design and applications; 2018; Springer. p. 821–831.
[39] Long W, Cai S, Jiao J, et al. An efficient and robust grey wolf optimizer algorithm for large-scale numerical optimization. Soft comput. 2020;24:997–1026.
[40] Chen D, Zou F, Li Z, et al. An improved teaching-learning-based optimization algorithm for solving glo bal optimization problem. Inf Sci (Ny). 2015;297:171–190.
[41] Premkumar M, Kumar C, Sowmya R. Mathematical modelling of solar photovoltaic cell/panel/array based on the physical parameters from the manufacturer's datasheet. Int J Renew Energy Dev. 2020;9(1):7–22.
[42] Premkumar M, Subramaniam U, Babu TS, et al. Evaluation of mathematical model to characterize the performance of conventional and hybrid PV array topologies under static and dynamic shading patterns. Energies. 2020;13:3216.
[43] Madin LP. Aspects of jet propulsion in salps. Can J Zool. 1990;68(04):765–777.
[44] Anderson PAV, Bone Q. Communication between individuals in salp chains. II. Physiology. Proc of Royal Soc London. Ser B. Biological Sci. 1980;210(1181):559–574.
[45] Andersen V, Nival P. A model of the population dynamics of salps in coastal waters of the Ligurian sea. J Plankton Res. 1986;8(6):1091–1110.
[46] Henschke N, Smith JA, Everett JD, et al. Population drivers of a Thalia democratica swarm: insights from population modelling. J Plankton Res. 2015;37(05):1074–1087.
[47] Premkumar M, Dhanasekar N, Dhivakar R, et al. Comparison of MPPT algorithms for PV system-based DC-DC converter. Adv Nat Appl Sci. 2016;17(9):212–221.
[48] Premkumar M, Sumithira TR. Design and implementation of new topology for non-isolated dc-dc micro-converter with effective clamping circuit. J Circuits Syst Comput. 2018: 1–22. doi:10.1142/S0218126619500828.